HHS Public Access

Author manuscript

*Nat Immunol*. Author manuscript; available in PMC 2013 January 04.

Published in final edited form as:

*Nat Immunol*. 2010 November ; 11(11): 1014–1022. doi:10.1038/ni.1944.

# Interleukin 37 is a fundamental inhibitor of innate immunity

**Marcel F Nold**[1,2], **Claudia A Nold-Petry**[1,2], **Jarod A Zepp**[1], **Brent E Palmer**[1], **Philip Bufler**[3], and **Charles A Dinarello**[1]

[1]Department of Medicine, University of Colorado Denver, Aurora, CO 80045, USA

[2]The Ritchie Centre, Monash Institute of Medical Research, Monash University, 3168 Melbourne, Victoria, Australia

[3]Children's Hospital, Ludwig-Maximilians University, 80337 Munich, Germany

## Abstract

The function of interleukin 37 (formerly IL-1 family member 7) remains elusive. Expression of IL-37 in macrophages or epithelial cells imparted near complete suppression of pro-inflammatory cytokines, whereas the abundance of these cytokines increased with silencing of endogenous IL-37 in human blood cells. Anti-inflammatory cytokines remained unchanged under similar conditions. IL-37-transgenic mice were protected from lipopolysaccharide-induced shock, exhibiting markedly improved lung and kidney function and reduced liver damage. IL-37-transgenic mice had less circulating and tissue cytokines (72-95% lower) than wild-type mice and exhibited less dendritic cell activation. IL-37 interacted intracellularly with Smad3 and IL-37-expressing cells and transgenic mice exhibited less cytokine suppression when endogenous Smad3 was depleted. IL-37 thus emerges as a natural suppressor of innate inflammatory and immune responses.

---

The interleukin 1 (IL-1) family of ligands comprises 11 members; most are pro-inflammatory. The receptors, signaling pathways, and functions of the classical family members (IL-1α [http://www.signaling-gateway.org/molecule/query?afcsid=A004200] and IL-1β [http://www.signaling-gateway.org/molecule/query?afcsid=A003663], IL-18) have been studied extensively. Among the more recently described IL-1 family cytokines, IL-33 (also called IL-1F11) stands apart, as it is the long-sought ligand for the IL-1 receptor family member ST2 (ref. [1]). Knowledge of IL-1F7, on the other hand, which was first identified by *in silico* research in 2000 (summarized in[2]) remains limited. With the exception of IL-18 and IL-33, the entire human *IL1* family maps to the IL-1 family cluster of genes on chromosome 2 (ref. [2]). Comprising 12 β-barrel strands, IL-1F7 shares the structural pattern of the IL-1 family but particularly that of IL-18 (ref. [3]). Although constitutive IL-1F7 mRNA is found

---



Correspondence should be addressed to Charles A Dinarello, M.D.; University of Colorado Denver, Division of Infectious Diseases; 12700 E 19th Ave, B168; Aurora, CO 80045; Phone 303-724-6172; Fax 303-724-6178; cdinarello@mac.com.

**Author Contributions**: MFN, CANP, PB, and CAD designed the study, analyzed the data, and wrote the manuscript. MFN, CANP, JAZ, and PB did experiments. BEP was in charge of the flow-cytometry analysis.

The authors have no conflicting financial interests.

in the testis, thymus and uterus, IL-1F7 is inducible in peripheral blood mononuclear cells (PBMCs) and dendritic cells[4]. The protein has been reported in monocytes[5], tonsil plasma cells, and breast carcinoma cells[6]. Five splice variants exist (IL-1F7a through e)[4, 7-10], with IL-1F7b (NM014439) being the largest and is comprised from 5 of the 6 exons. None of the isoforms contain a typical signal peptide, but IL-1F7b and IL-1F7c each contain exons 1 and 2, and exon 1 encodes a putative caspase-1 [http://www.signaling-gateway.org/molecule/query?afcsid=A000492] cleavage site. In addition, IL-1F7b can form homodimers[6]. Interestingly, IL-1F7 is the only IL-1 family member for which a murine homologue has yet to be found.

Processing by caspase-1 cleaves the recombinant (r)IL-1F7b precursor into mature IL-1F7b[6]. Both the precursor and mature rIL-1F7b are reported to bind to the IL-18 receptor α chain (IL-18Rα) as demonstrated by immunoprecipitation assays of IL-18Rα:Fc constructs. However, the affinity of IL-18 itself for IL-18Rα is approximately 50 times higher than that of mature rIL-1F7b[6]. Although mature IL-1F7b binds to IL-18Rα:Fc, rIL-1F7b did not antagonize the activities of IL-18 such as induction of interferon γ (IFN-γ)[5,6] and thus is not a receptor antagonist for IL-18 (ref. [5]). However, consistent with the binding of rIL-1F7b to IL-18Rα, IL-1F7b forms a complex with IL-18 binding protein (IL-18BP [http://www.signaling-gateway.org/molecule/query?afcsid=A001254])[5], the natural antagonist of IL-18 (ref. [11]). Lower concentrations of IL-18BP inhibit IL-18 activity more effectively than higher concentrations[12], which may be attributable to complex formation between IL-1F7b and IL-18BP. Previously, we reported that mature IL-1F7b translocates into the nucleus and that this process was dependent on caspase-1 (ref. [13]). We therefore proposed that IL-1F7b may act as a cytokine with intracellular as well as extracellular functionality.

Here, we present the functional role and mechanism of action for IL-1F7. To accomplish this, we either reduced IL-1F7 expression in human PBMCs with siRNA or expressed the cytokine in human macrophages, epithelial cells, and mouse macrophages. Moreover, a mouse strain transgenic for IL-1F7b was generated and subjected to non-lethal endotoxic shock, in which heterozygotes and homozygotes were studied. From the data presented here, IL-1F7 emerges as a natural inhibitor of immune responses. Because of the fundamental nature of these effects, we propose this member of the IL-1 family to be assigned the name IL-37.

## Results

### Regulation and function of endogenous IL-37

Regulation and function of endogenous IL-37 are unknown. First, steady-state constitutive and inducible IL-37 protein abundance was assessed in PBMCs (Fig. 1a). The TLR ligands lipopolysaccharide (LPS) and $Pam_3CSK_4$ as well as transforming growth factor $\beta_1$ (TGF-$\beta_1$) were highly effective in inducing IL-37 (Fig. 1a, left). IL-18, IFN-γ, IL-1β, tumor necrosis factor (TNF), and CpG also increased synthesis, whereas IL-4 plus granulocyte-macrophage colony-stimulating factor (GM-CSF) inhibited constitutive IL-37 expression.

To assess the function of endogenous IL-37, PBMCs from seven donors were transfected with concentration-matched pairs of scrambled siRNA or siRNA to IL-37 (siIL-37). IL-37 protein abundance in LPS-stimulated PBMCs was considerably reduced by specific siRNA (Fig. 1b). In the same cells, treatment with siIL-37 consistently resulted in dose-dependent 2- to 3-fold increases in production of mature IL-1β, IL-6, and TNF in PBMCs stimulated with either LPS or $Pam_3CSK_4$ (Fig. 1c,d, and Supplementary Fig. 1a). PBMCs were also stimulated with the TLR6-TLR2 ligand MALP-2, which resulted in a comparable pattern (data not shown). In contrast, anti-inflammatory IL-10 and IL-1Ra expression in these same supernatants were unaffected by siIL-37 treatment (Fig. 1e and Supplementary Fig. 1b). The effect of reducing endogenous IL-37 in LPS-stimulated PBMCs was further investigated using an array of 36 cytokines (Fig. 1f). The array confirmed the results described above; moreover, the array revealed changes in protein abundance of IL-1α (50% increased) as well as GM-CSF and G-CSF (2.1- and 2.4-fold increases, respectively).

To demonstrate the expression of IL-37 in human disease, synovial tissue from patients with active rheumatoid arthritis were subjected to immunohistochemistry. Diseased synovial lining contained large amounts of IL-37 (Fig. 1g).Thus, we found that production of IL-37 is induced through pattern-recognition and cytokine stimulation and that endogenous IL-37 is a response that limits runaway inflammation initiated by innate pathways.

## IL-37 abrogates pro-inflammatory cytokines in RAW cells

Using a mouse macrophage RAW cell line which stably expresses the human IL-37b isoform (IL-1F7b, in keeping with the splice variant nomenclature)[5,14], termed RAW-IL-37, we observed that the cytokine was expressed constitutively at low amounts, whereas protein expression dose-dependently increased upon stimulation with LPS (Fig. 2a, left). In RAW cells, the molecular weight of IL-37b was 25 kDa; however, endogenous IL-37 in PBMCs migrated at a molecular weight of approximately 45 kDa (Fig. 1a). As the immunoblots were performed under non-reducing conditions, this result is likely due to homodimerization[6]. We ascertained specificity of the IL-37 antibody by depletion using excess recombinant IL-37b (Fig. 1a, right).

Having confirmed that IL-37b was highly effective in reducing LPS-stimulated TNF, MIP-2, and IL-1α (Fig. 2b-d) as compared to mock-transfected RAW cells, we performed an array of 40 mouse cytokines, chemokines, and other inflammatory mediators. In RAW-IL-37 cells, several major cytokines such as IL-1α (by 88%) and IL-6 (86%) were almost completely suppressed in (Fig. 2e). Production of M-CSF, BCA-1, GM-CSF, and IL-1β was considerably (55 - 62%) reduced, and MCP-5, IL-23, and IL-1Ra, were also lower. The mean changes in other molecules were below 30% (Fig. 2e). Stimulation of RAW-IL-37 cells with IL-1β or TNF revealed similar reductions in IL-1α, TNF, and MIP-2 expression (data not shown).

Various TLR ligands induced IL-37b in RAW-IL-37 cells (Fig. 2a, right). Pronounced reductions in IL-1α, MIP-2, TNF, and IL-6 expression (by up to 99, 97, 92, and 98%, respectively) also occurred in RAW-IL-37 cells when stimulated by various TLR ligands (Supplementary Table 1). Therefore, expression of IL-37b in murine RAW macrophages reduced TLR-induced pro-inflammatory cytokines.

### IL-37 reduces cytokines in monocytic and epithelial cells

The human monocytic cell line THP-1 was transiently transfected with a pIRES vector controlled by a constitutively active cytomegalovirus (CMV) promoter that contained full-length IL-37b linked to a FLAG tag at its carboxyl terminus. The vector also contained a green fluorescence protein (GFP)-coding sequence. IL-37b expression significantly reduced spontaneous and LPS-induced IL-1α, IL-1β, TNF, and IL-8 expression in undifferentiated (Fig. 3a,b and Supplementary Fig. 2a) and phorbol ester (PMA)-differentiated[15] THP-1 cells (Fig. 3c and Supplementary Fig. 2b,c). This suppression was also observed for IL-1β-induced expression of IL-1α, IL-8, and TNF (Fig. 3b,c and Supplementary Fig. 2a,c).

Steady-state IL-37 mRNA is found in tissues rich in epithelial cells[4]. Hence, we transfected the epithelial cell line A549 with the pIRES-IL-37b plasmid (immunofluorescence in Supplementary Fig. 2d, immunoblot in Fig. 3d). Constitutive and IL-1β-induced IL-6 and IL-1α production were reduced by 43 and 47% and 34 and 42%, respectively (Fig. 3e,f). The reduction of IL-1β- and LPS-induced pro-inflammatory cytokines in human monocytes and macrophages as well as in epithelial cells is consistent with the data obtained by vector-mediated expression of IL-37b in RAW cells and also by silencing endogenous IL-37 in primary human blood mononuclear cells.

### Smad3 and IL-37 form a functional complex

In a proteomics-based search for proteins interacting with Smad3, IL-37 was listed[16]. Therefore, we transfected human A549 cells with FLAG-tagged IL-37b and observed that IL-37b co-localized with phospho-Smad3 by immunofluorescence (Fig. 4a, bright yellow in the overlay). Both IL-37b and phospho-Smad3 were induced by IL-1β and most prominently stained in perinuclear and cytosolic regions. Images of the corresponding controls (mock-transfected cells) are shown in Supplementary Fig. 3. Furthermore, IL-37b-Smad3 complex formation was demonstrated by anti-FLAG immunoprecipitation (Fig. 4b). The occurrence of more than one band is likely due to alternate splicing of Smad3 (ref. [17]).

Next, we tested the hypothesis that Smad3 is required for IL-37 activity. We used the specific inhibitor SIS3 (ref. [18]) to block Smad3 activation and observed a dose-dependent reversal of the inhibition of IL-6 and IL-1α expression in the LPS-stimulated RAW-IL-37 cells (Fig. 4c and Supplementary Fig. 4). Under the same conditions, the effects of SIS3 in mock-transfected RAW cells were absent. We then evaluated the IL-37b-Smad3 interactions in THP-1 cells. The SIS3-induced increases in IL-1β expression were significantly greater when high concentrations of IL-37b were present (Fig. 4d). By immunofluorescence, there was similar colocalization of IL-37b and Smad3 in THP-1 cells as observed in A549 cells (data not shown).

We then generated stable THP-1 clones depleted of Smad3 by lentiviral shRNA coding for Smad3 (mRNA reduction to roughly 12% of that of scrambled siRNA-transfected clones (data not shown), protein knockdown shown in Supplementary Fig. 5). In these cells, the ability of IL-37b to reduce IL-1β- or LPS-induced production of IL-8 (Fig. 4e), IL-6, and TNF (not shown) was considerably reduced. These *in vitro* findings were confirmed *in vivo* as described below.

### Post-receptor signal transduction in the presence of IL-37

We determined activation of 37 different kinases triggered by treatment of LPS plus IFN-γ in THP-1 cells transfected with IL-37b. Regulators of cellular adhesion and migration, namely focal adhesion kinase (FAK), proline-rich tyrosine kinase 2 (Pyk2), and paxillin, were suppressed by up to 78% (Supplementary Fig. 6). Mitogen-activated protein (MAP) kinase p38α was reduced by 51% and expression of multiple STAT transcription factors, hematopoietic cell kinase (Hck), p53, and target of rapamycin (TOR) were also lower in IL-37b-transfected cells as compared to controls. Because changes in kinases affect cellular proliferation and differentiation, we assessed live-cell images from RAW-IL-37 and mock-transfected RAW cells. We observed striking morphological differences in cells transfected with IL-37b. For example, whereas mock-transfected RAW cells formed pseudopodia, RAW-IL-37 hardly did so (Supplementary Fig. 7a (arrows) and b). Moreover, stimulation with LPS induced considerable vacuolization in most mock-transfected cells (Supplementary Fig. 7c, arrows), but not in RAW-IL-37. Similar results were obtained when the cells were treated with TLR ligands 1 to 6 and 9 (data not shown). We therefore demonstrate that IL-37b regulates post-receptor signal transduction in a specific fashion and that these effects result not only in a reduction of pro-inflammatory cytokine production, but also in morphological changes in RAW cells.

### IL-37 protects mice from LPS-induced shock

To investigate whether IL-37 suppresses innate responses to LPS *in vivo*, we generated a line of mice transgenic for FLAG-tagged IL-37b (IL-37tg). The presence or absence of IL-37b protein expression in IL-37tg or PCR-negative littermates (neg) was confirmed by FLAG immunoprecipitation and IL-37 staining of splenocytes as well as by IL-37 immunoblots on white blood cell lysates (Fig. 5a,b). We observed that, similar to *in vitro* results, uninduced, steady-state production of IL-37b *in vivo* was low despite the constitutively active CMV promoter. Synthesis of IL-37b was augmented by LPS administration. Outside of experimental settings, the IL-37tg colony did not differ from negative or wild-type mice: growth, behavior, reproduction, and male-to-female ratio were equal over many generations.

We induced non-lethal endotoxic shock in IL-37tg, negative littermates, and wild-type mice with 10 mg/kg LPS injected i.p. The various parameters assessed did not reveal differences between negative littermates and wild-type mice; thus, these two groups are shown as one (hereafter designated as neg-WT). To establish normal values in this model, additional mice from each group received vehicle only. In this latter group, we found no difference in any parameter between IL-37tg and neg-WT. Compared to neg-WT, the effects of endotoxemia were markedly attenuated in the IL-37tg mice (Fig. 5c-k). LPS-induced hypothermia was less in IL-37tg, with the effect being most pronounced in homozygotes (Fig. 5c). IL-37tg mice also achieved respiratory compensation of the metabolic acidosis induced by LPS. For example, pH and $HCO_3$ were higher, $pCO_2$ was lower, and the base excess (BE) was less negative in IL-37tg than in neg-WT mice (Fig. 5d-g). IL-37tg mice were less dehydrated, as blood Na concentrations were not significantly different from vehicle-controls (Fig. 5h). Likewise, IL-37b conferred protection from a rise in potassium concentrations which in neg-WT mice reached nearly 6 mmol/l after LPS challenge (Fig. 5i). Moreover, LPS-induced

liver damage, as measured by increased alanine aminotransferase (ALT), was prevented in IL-37tg as the plasma activity of this enzyme was close to that in vehicle-injected control animals (Fig. 5j). Similar results were obtained for aspartate aminotransferase (AST) (Fig. 5k).

These physiological findings in IL-37tg mice were accompanied by a reduction of various cytokines in different compartments as compared to control mice similarly challenged by LPS (Figs. 6,7). In the plasma, reduced concentrations (up to 65% reduction compared to controls) of IL-6, IL-1β, IL-17, and IFN-γ were seen in heterozygous IL-37tg mice, whereas in homozygotes these cytokines were nearly absent (72 to 95% reduction, Fig. 6b,c). A cytokine protein array analysis revealed that 18 cytokines were reduced by more than 33% in IL-37tg, 16 of which were pro-inflammatory (Fig. 6a). Among the cytokines that were found in similar abundance in the plasma of IL-37tg and neg-WT were the anti-inflammatory I-309, IL-13, and IL-10. These findings, together with the finding that IL-4 and IL-27 averaged up to 2.5-fold increased concentrations in the plasma of IL-37tg mice, demonstrate IL-37b expression results in a specific modulation of the immune response to LPS. Importantly, these data are highly consistent with the suppression of cytokine production in cells transfected with IL-37b.

The amounts of pro-inflammatory cytokines and chemokines in the spleens and lungs of IL-37tg mice were also lower than in organs from neg-WT mice (Figs. 6d,e and 7a). With the exception of splenic expression of IL-1α, the pattern of cytokine regulation in the organs and the systemic circulation was similar. Interestingly, as opposed to the pro-inflammatory cytokines, the immunosuppressive TGF-$\beta_1$ was not reduced, but 1.8-fold increased in the spleens of IL-37tg mice.

Since the anti-inflammatory activity of IL-37b was not limited to cytokines of innate immunity, we determined whether IL-37b affected the function of dendritic cells (DCs), which serve as coordinators of immune responses. Among the splenocytes from the same mice shown in Fig. 6, we identified $CD11c^+$ DCs and assessed their activation status by measuring the surface expression of CD86 (B7-2, a co-stimulatory molecule that facilitates T cell activation) and MHC class II (a stimulator of $CD4^+$ T cells). We observed that the presence of IL-37b conferred a marked reduction in LPS-induced DC activation (Fig. 7b,c). Whereas in LPS-injected neg-WT mice the average expression of CD86 and MHC II on DCs was 73% with a range from 46 to 89%, IL-37tg homozygotes only averaged 47% $CD86^+$MHC $II^+$ with a range from 18 to 69%, indicating that considerably fewer DCs were activated in IL-37tg. Consistent with previous data (e.g.[19]), DCs in vehicle-treated mice were about 40% $CD86^+$MHC $II^+$ with no difference between neg-WT, IL-37tg heterozygotes, and IL-37tg homozygotes. Thus, IL-37b reduced the number of activated DCs to near constitutive background. We also measured activation of macrophages, which exhibited similar, but less pronounced inhibition (data not shown). Total numbers of DCs, macrophages ($F4/80^+$), NK cells ($NK1\text{-}1^+$), and $CD4^+$ T cells were similar in all strains and experimental conditions (not shown).

In cultures of fresh whole blood from the mice, we found that production of IL-6 and TNF induced by LPS, LPS plus IL-12, IL-1b, TNF, and IL-12 plus IL-18 were up to 86% lower

in IL-37tg than in neg-WT (Fig. 7d,e). Hence, the anti-inflammatory functions of IL-37 are also observed in various conditions *in vivo*. By suppressing pro- but sparing anti-inflammatory cytokines and by inhibiting DC activation, IL-37b protected the lung, kidney, and liver in a model of endotoxic shock.

### Smad3 *in vivo*-knockdown reduces the activity of IL-37

To demonstrate that Smad3 contributes to the function of IL-37 *in vivo*, we silenced Smad3 in the lungs of IL-37tg and neg-WT mice. Effective knockdown was determined by immunoblotting (Fig. 8a). Cytokine assays on the same lysates demonstrated that the anti-inflammatory function of IL-37 was considerably reduced when Smad3 was silenced (Fig. 8b,c). Whereas IL-1β protein abundance was 94% lower in IL-37tg mice compared to controls when scrambled siRNA was inhaled, this reduction was only 63% when Smad3 was silenced. For IL-17 expression, IL-37b-mediated reduction of protein concentrations was from 40.4 to 5.8 pg/mg total protein (86%) with scrambled siRNA, but only 53.3 to 35.7 pg/mg total protein (33%) with siRNA to Smad3. The effect of siRNA to Smad3 was a 1.5- to 2.4-fold increase in cytokine production in neg-WT, compared to an up to 15-fold increase in IL-37tg. These experiments corroborate the functional link between IL-37 and Smad3 but also are relevant to the anti-inflammatory portfolio of TGF-β.

## Discussion

Since the first description of IL-37 (IL-1F7) in 2000 (ref [8]), there has been no report on the function of endogenous IL-37. In the present study, reduction of IL-37 protein synthesis in PBMCs with specific siRNA increased the production of several pro-inflammatory mediators, among these IL-1α, IL-1β, IL-6, IL-12, G-SCF, GM-CSF, and TNF. Remarkably, expression of the anti-inflammatory IL-1Ra and IL-10 in the same cultures was unaffected. These data suggest that IL-37 acts as a negative feedback inhibitor of inflammatory responses and that this function is not dependent on anti-inflammatory cytokines such as IL-10. Since several TLR ligands as well as IL-1β, TNF, IFN-γ, and IL-18 induce IL-37, the siRNA data suggest that the mitigating activity of this cytokine affects a wide spectrum of inflammatory assaults. It is not unexpected that inflammation induces anti-inflammatory mechanisms in order to limit damage. Therefore, the observations that, in general, IL-37 is not constitutively expressed in tissues from healthy subjects but expression is high in synovial tissue from patients with rheumatoid arthritis are in accord with the concept that the function of IL-37 constitutes a negative feedback mechanism to curb excessive inflammation.

Unexpectedly, low concentrations of the immunoregulatory cytokine TGF-$\beta_1$ were effective in inducing endogenous IL-37, which is relevant to the interaction of IL-37 with Smad3. In a study designed to identify intracellular candidates that bind to Smad3 using two-dimensional gel electrophoresis and mass spectrometry, the only cytokine among the proteins binding Smad3 was IL-37 (ref. [16]). Smad proteins are the major intracellular signaling effectors of TGF-β and are phosphorylated by TGF-β receptors upon binding the ligand. Following phosphorylation, Smad3 translocates to the nucleus and affects gene transcription. For example, Smad3 binding to DNA inhibits DC and macrophage activation[20, 21], skews T

cells towards tolerance[22] or inhibits cellular cytotoxicity[23]. We previously demonstrated that IL-37b translocates to the nucleus[13] and in the present study, we observed that IL-37b binds to both non-phosphorylated and phosphorylated Smad3 in A549 and THP-1 cells by immunofluorescence and immunoprecipitation, each of which is consistent with the intracellular complex of Smad3-IL-37 identified by mass spectrometry[16]. The functionality of this complex was tested by using a specific inhibitor of Smad3 in RAW and THP-1 cells and siRNA to Smad3 *in vitro*. *In vivo*, silencing endogenous Smad3 significantly reduced the anti-inflammatory properties of IL-37b.

We conclude that IL-37 functions, at least in part, with Smad3, thus facilitating the known cytokine-suppressing properties of TGF-β[24]. Foremost, TGF-β is well established as a major inhibitor of DC function. For example, TGF-β and the downstream activation of the Smad pathway were required for Treg-mediated suppression of DC function, including expression of CD86 and production of pro-inflammatory cytokines, in a murine leukemia model[25]. In three other studies, blockade of TGF-β resulted in reduced capacity of antigen presentation[26] or costimulation[27] in human DC *in vitro*; also, treatment with TGF-$\beta_1$ caused a reduction of IL-12 production and a reduced stimulation of T-cell proliferation by human monocyte-derived DCs[28]. *In vivo*, functional inactivation of the TGF-β receptor (and hence TGF-β signaling) in DCs resulted in increased production of $T_H1$ and $T_H17$ cytokines and aggravation of autoimmune encephalomyelitis[29]. These data concur with IL-37b-mediated suppression of DC function as well as cytokine regulation, the latter including the elimination of the low background expression of natural IL-37 by IL-4/GM-CSF and the pronounced effect of IL-37 on GM-CSF.

The concept that IL-37 acts via an intracellular mechanism in translocating to the nucleus is not new in cytokine biology. For example, IL-1α is found in the nucleus and affects the transcriptional machinery[30, 31]. IL-33 also functions as an endothelial transcription factor[32]. Outside the IL-1 family, IL-16 (ref. [33]), HMGB-1 (ref. [34]), and MIF[35] are examples for cytokines with intracellular activities. However, these cytokines also exhibit a second function; released from the cell, they trigger their cognate cell surface receptor. Thus, these molecules reveal a dual mode of action. Although recombinant IL-37 has been reported to bind to IL-18Rα[4, 6], IL-37 does not appear to function as a receptor antagonist for IL-18. However, in the presence of low concentrations of IL-18 binding protein, recombinant IL-37 reduces IL-18-induced IFN-γ[5].

As anticipated from the increases in pro-inflammatory cytokines with siRNA-mediated inhibition of endogenous IL-37, several LPS- and IL-1β-induced pro-inflammatory cytokines were markedly decreased in human and murine macrophages; the cell type in which most previous studies on IL-37 were conducted[4-6, 13, 14]. Since IL-37 is naturally expressed in organs comprising epithelial cells[4, 6], we transfected human lung epithelial cells and confirmed that IL-37 was active in this model. This extension of IL-37 activity to now also including IL-1-mediated signals in epithelia is important, as IL-1β stimulation and downstream effector functions of IL-6 constitute major pro-inflammatory insults for epithelial cells[36].

Despite the constitutively active CMV promoter, IL-37b protein amounts were low under steady-state conditions *in vitro* and *in vivo*, but markedly increased with an inflammatory challenge Consequently, IL-37b-mediated reductions in cytokines were also only observed during inflammation. This observation is consistent with the presence of a coding region instability element in IL-37b mRNA, which is overcome by exogenous stimulation, resulting in mRNA stabilization and IL-37b protein production[14]. We therefore infer that the suppression of pro-inflammatory cytokines by IL-37 is undesirable under resting conditions and for the early stages of innate immune responses, but that later, when increasing danger is sensed, expression of IL-37 prevents an excessive inflammatory response.

Among the kinases whose phosphorylation was suppressed by IL-37b expression were STATs 1-4, which are involved in signal transduction of various pro-inflammatory cytokines, for example IL-6, IL-12, and IFN-γ[37]. Thus, their deactivation represents a straightforward mechanism utilized by IL-37 to attenuate inflammation; furthermore, this notion is in accord with a functional IL-37-Smad3 complex, as Smad3 mostly antagonizes STAT1 and STAT3 (examples in[38, 39], respectively). The same is valid for the reduction of c-Jun, which is a part of the IL-1-inducible pro-inflammatory transcription factor AP-1 (ref. [40]) and is inhibited by TGF-β[41]. Expression of IL-37b also reduced phosphorylation of p38 MAPK which holds a central position in several, predominantly pro-inflammatory signaling cascades[42]. Furthermore, GSK-3α/β phosphorylation is increased by IL-37b expression, rendering this kinase inactive. Remarkably, such inhibition of GSK-3 activity skews TLR-ligand-triggered monocytes away from secreting pro-inflammatory cytokines and towards producing IL-10 (ref. [43]).

To assess IL-37 *in vivo*, we generated a mouse strain transgenic for human IL-37b. Both heterozygous and homozygous IL-37tg mice were protected from non-lethal LPS-induced endotoxic shock, as demonstrated by less severe disease in lung, kidney, and liver and reduced hypothermia, although most of the effects were more pronounced in homozygotes. This protection was afforded through a marked reduction in the amount of pro-inflammatory cytokines in lungs, spleens, and plasma, as well as through suppression of DC activation by IL-37b, and was, at least in part, mediated by Smad3. These data provide evidence that IL-37 plays a major role *in vivo*. Intriguingly, these findings resemble a report which asserted an essential role for TGF-β and Smad3 in the protection from excessive inflammation following an endotoxin challenge[44]. In that study, TGF-$\beta_1^{-/-}$ and Smad3$^{-/-}$ mice featured higher expression of IL-1β, TNF, and iNOS in liver, lung, and heart tissue, as well as increased NF-κB activation and higher NO plasma levels, ultimately resulting in hyperresponsiveness to LPS. The similarities between these data and our results indicate that the IL-37-Smad3 complex is relevant *in vivo*.

To assess whether the protective functions of IL-37 extend beyond LPS in a whole animal model as they did *in vitro*, we stimulated whole blood from IL-37tg and control mice with IL-1β, TNF, IL-12 plus IL-18, and IL-12 plus LPS. We found that the pro-inflammatory effect of each of the stimuli was markedly suppressed by IL-37b. Together with the Smad3-associated mechanism of action, these findings are consistent with the inhibition of DC function conferred by IL-37b. DCs receive, integrate, and pass on signals from and to a wide variety of cells and thus constitute part of the interface of innate and adaptive immunity. It is

likely that by reducing surface expression of the costimulatory molecule CD86 (B7-2) and MHC II (a major activator of $CD4^+$ T-cells) on DCs along with propagating an anti-inflammatory cytokine environment, IL-37 attenuates T-cell responses. The suppression of DC activation *in vivo* is also concordant with the IL-37-mediated inhibition of M-CSF and GM-CSF and the reduction of RAW cell differentiation and activation.

We conclude that endogenous IL-37 suppresses immune responses by shifting the cytokine equilibrium away from excessive inflammation. This is achieved at least in part by inhibition of DC activation on the cellular level and by interaction with Smad3 and modulation of kinase-checkpoints on the molecular level. The protective activity of IL-37 can be observed *in vitro* as well as *in vivo* and affects a broad spectrum of pro-inflammatory insults such as TLR ligands, IL-1β, TNF, and IL-12 plus IL-18, placing this cytokine as a new member in the portfolio of classical anti-inflammatory cytokines, such as IL-10 and TGF-β.

## Methods

### Cell culture and transfections

Stable transfection of RAW264.7 cells with an IL-37b (IL-1F7b) or a mock construct under a constitutively active CMV promoter were previously described and are termed RAW-IL-37 or mock-transfected[14]. Since RAW-IL-37 replicated slower than mock-transfected, cytokine data were normalized to total protein by the formula: raw cytokine data in pg/ml/ total protein concentration in the lysate in mg/ml.

For transfection of human THP-1 and A549 cells, IL-37b was inserted into a pIRES vector with a GFP expression sequence, and the C-terminus of IL-37b was ligated to FLAG. The promoter controlling expression was identical to that in pTARGET described above. The identical vector without the IL-37b insert (= mock-transfected) was also constructed. Cells were transfected using the Amaxa Nucleofector Kit V (THP-1) or T (A549) and program V001 or X001, respectively, followed by an overnight recovery.

To differentiate transfected THP-1 cells into macrophages, the medium contained PMA (50 ng/ml). 20 h after transfection, all cells were counted and plated. Undifferentiated cells were resuspended in RPMI with penicillin/streptomycin and 1% human serum and stimulated immediately, whereas differentiated cells were incubated for another 24 h with PMA and stimulated thereafter.

A549 cells were transferred into 6-well plates after transfection and cultured in F12/K medium supplemented with 10% FCS and 1% penicillin/streptomycin. On the next day, the cells were provided with fresh reduced serum (2%) F12/K and were stimulated.

For silencing of Smad3, $10^5$ THP-1 cells were incubated with $10^4$ lentiviral particles containing shRNA to Smad3 (Santa Cruz, catalog number sc-38376-V) or scrambled in 500 μl growth medium which contained 5 μg/ml polybrene. After 24 h, the cells received fresh medium without polybrene for an additional 3 days of incubation. Thereafter, 1 μg/ml

puromycin was added to the cultures. Cells surviving at least 1 week under these conditions were used in the experiments.

Experiments involving human blood were approved by the Colorado Multiple Institutional Review Board. PBMCs were isolated from peripheral venous blood of healthy volunteers by density gradient centrifugation. Electroporation with the Amaxa device was performed as described previously[45]. 100 nM siIL-37 (Thermo Fisher Scientific), which targeted all isoforms of IL-37, comprised 25 nM of the four following antisense sequences: I, uca agg aug agg cua aug cuu; II, caa ugu guu ucc ugu ucu cuu; III, uua caa uug cag gag gug cuu; IV, uua ucc uug uca cag uag auu (all 5′ to 3′). After overnight recovery, cells were incubated for 1 day with or without stimulation. Supernatants were then taken, cells were lysed in lysis buffer[45] and frozen at −80°C.

## Generation of IL-37tg mice

All mouse experiments were approved by the Colorado Multiple Institutional Review Board. The Declaration of Helsinki was respected. Fertilized eggs of C57BL/6 mice were injected with the pIRES IL-37b expression plasmid described in the previous section and implanted into C57BL/6 females. Male founders were mated with C57BL/6 wild-type females. IL-37tg were determined by genotyping PCRs for IL-37b performed on tails at 3 to 4 weeks of age. PCR-negative littermates (neg) and wild-type mice were used as controls.

## *In vivo* and whole blood experiments and splenocyte assays

24 h after i.p.-injection of LPS, IL-37tg or neg-WT were anesthetized and plasma was obtained by orbital bleeding into heparinized tubes. Blood was processed immediately for blood gas and liver enzyme analysis by the clinical laboratory of the University of Colorado Hospital. Cytokines were measured in plasma obtained by gentle centrifugation (300 g for 12 min).

For whole blood experiments, blood was obtained by puncture of the submandibular vein (first bleeding) or by orbital bleeding (second bleeding in conjunction with splenocyte isolation). A small aliquot was taken for white blood cell counts. The remaining whole blood was diluted 1:5 in RPMI and stimulated for 20 h. After this incubation, cultures were lysed with Triton X-100 (final 0.5%) and underwent a freeze-thaw cycle before cytokine determinations.

For isolation of splenocytes, spleens were removed, macerated, and passed through a 70 μm cell strainer. After several rinses with cold PBS, splenocytes were centrifuged, resuspended in RPMI with 5% FCS and 1% penicillin-streptomycin, plated, and used for experiments. For flow cytometry analysis, spleens were injected with 1 mg/ml collagenase IV (Worthington Biochemicals), cut into pieces, incubated at 37 °C for 30 min, strained, washed twice with PBS containing 1% BSA, counted, and stained as described below.

## Surface staining and flow-cytometry

Splenocytes ($5 \times 10^6$) were washed twice with PBS containing 1% BSA and incubated with an Fc-receptor blocking antibody (anti-CD16/32, eBioscience) for 15 minutes to reduce non-

specific staining. The splenocytes were then stained with anti-F4/80 (eFluor 450, clone BM8), anti-CD86 (APC, clone GL1), anti-MHC class II (Alexa Fluor 700, clone M5/114.15.2), anti-NK1-1 (PE, clone PK136), and appropriate isotype controls (eBioscience), as well as anti-CD4 (PE-Cy7, clone RM4-5), anti-CD11c (FITC, clone HL3), and appropriate isotype controls (all BD) for 30 min at 4°C. Cells were then washed twice and fixed with 1% formaldehyde.

Cells were analyzed using an LSR-II flow cytometer (BD Immunocytometry Systems). Between 0.5 and 1 million events were collected. Electronic compensation was performed with antibody capture beads (BD Biosciences) stained separately with individual antibodies used in the test samples. To ensure the accuracy and precision of the measurements taken from day to day quality control was performed on the LSR-II daily using the Cytometer Setup & Tracking (CS&T) feature within BD FACSDiva software. CS&T beads (BD Biosciences) were used to determine voltage, laser delays and area scaling and to track these settings over time. A manual quality control (QC) using rainbow beads was also performed daily to verify the laser delay and area scaling determined by CS&T. The data files were analyzed using the FlowJo Software (Treestar). Splenocytes were gated by their forward and side scatter profile. $CD11c^+$ cells were selected and expression of CD86 and MHC class II was analyzed using a bivariate dot plot with biexponential scaling. Quadrant gates were set using cells stained with isotype controls and the percentage of $CD11c^+$ cells expressing both CD86 and MHC class II was determined.

### *In vivo* siRNA and LPS inhalation

To achieve a complete inhalation, mice were anesthetized with isoflurane and observed closely. Immediately after cessation of breathing activity, mice were removed from the isoflurane environment, and the concentrated siRNA (10-15 μl), was pipetted onto the nostrils. LPS was inhaled similarly 20 h later. Anti-Smad3 siRNA (Thermo Fisher Scientific) contained equal parts of the following four target sequences: I, cca ugg agc ucu gug agu u; II, gca uug uac ccc auu guu a; III, ggg uca acc aug aag aug u; IV, gug gga acu uca aau gga a.

### Electrochemiluminescence (ECL) assays, ELISAs, and multiplex ELISAs

Cytokines were measured using one of three methods. 1. ECL: Specific antibody pairs and an Origen Analyzer (Wellstat Diagnostics) were used as described previously[45]. 2. Conventional ELISAs (R&D Systems) confirmed the ECL data and were used alone in the case of murine IFN-γ and TGF-$\beta_1$. 3. Murine plasma and tissues were subjected to multiplex ELISA (Quansys Biosciences) analysis. Both ELISA methods were performed as recommended by the manufacturers. Recombinant cytokines were obtained from R&D Systems.

### Immunoblot

IL-37 was detected using an affinity-purified rabbit polyclonal antibody[5] and a horseradish peroxidase-labeled goat anti-rabbit secondary antibody (Jackson Immunoresearch Laboratories). Equal loading was ascertained by determination of protein concentrations and/or β-actin staining. For the antibody-depletion experiments, excess recombinant IL-36

(1 μg/ml, R&D Systems) or vehicle was added to the IL-36 antibody, which was then incubated for 4 h. Identical samples were loaded on one gel, which was blotted. The membrane was then cut into two halves. One half was incubated with the depleted IL-36 antibody, the other half was incubated with the vehicle-treated antibody. Both blots were developed simultaneously.

### Immunoprecipitation

Cells were first washed with cold PBS, scraped into 100 μl NP-40 buffer, and homogenized. Immunoprecipitation was performed using an Anti-FLAG M2 affinity gel (Sigma). After elution with 0.1 M glycine-HCl pH 3.5 and neutralization with 0.5M Tris-buffer (pH 7.4), proteins were subjected to electrophoresis under non-reducing conditions, then transferred to nitrocellulose membranes (0.2 μm) and immunoblot analysis was performed as described above using a rabbit anti-human Smad3 antibody (clone C67H9, Cell Signaling Technology).

### Cytokine protein and phospho-kinase arrays

Equal volumes of supernatants or lysates were incubated with pre-coated cytokine or phospho-kinase array membranes, respectively (Proteome Profiler Arrays, R&D Systems). Densitometry was performed and percent changes in individual cytokines were calculated as follows: background-corrected od/mm$^2$ of IL-37b-expressing or siIL-37 dots divided by respective background-corrected od/mm$^2$ of mock-transfected or scrambled dots, respectively. Loading variability between separate membranes was controlled for by densitometry of the positive control spots, followed by normalization of the density of each cytokine to the mean density of these positive control spots. Total protein was also measured and differences in cell death were excluded by LDH measurements (data not shown).

### Photomicrographs and immunofluorescent microscopy

For colocalization experiments, A549 or THP-1 cells were transiently transfected with the IL-37b or the mock construct, then cultured in Lab-Tek II Chamber Slides (Nunc) for 24 h. Thereafter, the medium was changed, cells were rested for 2 h, and then either stimulated for 30 min with 10 ng/ml IL-1β or left untreated. Cells were then washed with cold PBS, fixed with methanol/acetone for 10 min, and blocked in 10% donkey serum/1% BSA in PBS for 1 h. An overnight incubation at 4°C with the primary antibodies (anti-human phospho-Smad3 (Ser$^{423/425}$, clone C25A9, Cell Signaling Technology) at 1:100 and anti-FLAG (M2, Sigma) at 1:100) was followed by 3 washes with PBS followed by a 1 h incubation in the dark with the respective secondary antibodies (Invitrogen) coupled to FITC or Cy3. Nuclei and all membranes were stained with DAPI and an Alexa Fluor 633 conjugate of WGA (both Invitrogen), respectively. After another 3 washes with PBS, Antifade was applied to the slides. Digital confocal imaging was performed on a Zeiss LSM 510 Meta system with Axiovert 200 in conjunction with the Coherent Chameleon excitation laser.

### Statistical analysis

Datasets (raw data) were first tested for normality and equal variance (*P*-value to reject = 0.05) using SigmaStat (Systat Software Inc.). Thereafter, the appropriate statistical test was

applied (all one-tailed): cell culture experiments: unpaired *t*-test ($\alpha = 0.05$) or Mann-Whitney rank sum test; transgenic mice: unpaired *t*-test ($\alpha = 0.05$), rank sum test, one way ANOVA, or one way ANOVA on ranks.

## Supplementary Material

Refer to Web version on PubMed Central for supplementary material.

## Acknowledgments

We are grateful for the advice regarding immunofluorescence from F. Gamboni-Robertson and F. Eckerdt (both UCDenver). We also thank T. Azam, T. Goncharov (both UCDenver), and M. Fink (Ludwig Maximilians University Munich) for excellent assistance. We thank L. Joosten (Radboud University Nijmegen) for performing the immunohistochemistry, D. Finkel (R&D Systems) for providing assistance regarding the protein arrays, and P. Pagel (University of Technology Munich) for the comprehensive data base research for IL-37-interacting molecules. This work was supported by NIH grants AI-15614 and CA-04 6934 to CAD as well as by the Deutsche Forschungsgemeinschaft grants No 747/1-1 to MFN and Bu 1222/3-1, 3-2, and 3-3 to PB.

## References

1. Schmitz J, et al. IL-33, an interleukin-1-like cytokine that signals via the IL-1 receptor-related protein ST2 and induces T helper type 2-associated cytokines. Immunity. 2005; 23:479–490. [PubMed: 16286016]
2. Dunn E, Sims JE, Nicklin MJ, O'Neill LA. Annotating genes with potential roles in the immune system: six new members of the IL-1 family. Trends Immunol. 2001; 22:533–536. [PubMed: 11574261]
3. Priestle JP, Schar HP, Grutter MG. Crystallographic refinement of interleukin 1 beta at 2.0 A resolution. Proc Natl Acad Sci USA. 1989; 86:9667–9671. [PubMed: 2602367]
4. Pan G, et al. IL-1H, an interleukin 1-related protein that binds IL-18 receptor/IL-1Rrp. Cytokine. 2001; 13:1–7. [PubMed: 11145836]
5. Bufler P, et al. A complex of the IL-1 homologue IL-1F7b and IL-18-binding protein reduces IL-18 activity. Proc Natl Acad Sci USA. 2002; 99:13723–13728. [PubMed: 12381835]
6. Kumar S, et al. Interleukin-1F7B (IL-1H4/IL-1F7) is processed by caspase-1 and mature IL-1F7B binds to the IL-18 receptor but does not induce IFN-gamma production. Cytokine. 2002; 18:61–71. [PubMed: 12096920]
7. Busfield SJ, et al. Identification and gene organization of three novel members of the IL-1 family on human chromosome 2. Genomics. 2000; 66:213–216. [PubMed: 10860666]
8. Kumar S, et al. Identification and initial characterization of four novel members of the interleukin-1 family. J Biol Chem. 2000; 275:10308–10314. [PubMed: 10744718]
9. Smith DE, et al. Four new members expand the interleukin-1 superfamily. J Biol Chem. 2000; 275:1169–1175. [PubMed: 10625660]
10. Taylor SL, Renshaw BR, Garka KE, Smith DE, Sims JE. Genomic organization of the interleukin-1 locus. Genomics. 2002; 79:726–733. [PubMed: 11991723]
11. Novick D, et al. Interleukin-18 binding protein: a novel modulator of the Th1 cytokine response. Immunity. 1999; 10:127–136. [PubMed: 10023777]
12. Nold M, et al. IL-18BPa:Fc cooperates with immunosuppressive drugs in human whole blood. Biochem Pharmacol. 2003; 66:505–510. [PubMed: 12907250]
13. Sharma S, et al. The IL-1 Family Member 7b Translocates to the Nucleus and Down-Regulates Proinflammatory Cytokines. J Immunol. 2008; 180:5477–5482. [PubMed: 18390730]
14. Bufler P, Gamboni-Robertson F, Azam T, Kim SH, Dinarello CA. Interleukin-1 homologues IL-1F7b and IL-18 contain functional mRNA instability elements within the coding region responsive to lipopolysaccharide. Biochem J. 2004; 381:503–510. [PubMed: 15046617]

15. Lai JP, et al. Full-length and truncated neurokinin-1 receptor expression and function during monocyte/macrophage differentiation. Proc Natl Acad Sci USA. 2006; 103:7771–7776. [PubMed: 16675550]
16. Grimsby S, et al. Proteomics-based identification of proteins interacting with Smad3: SREBP-2 forms a complex with Smad3 and inhibits its transcriptional activity. FEBS Lett. 2004; 577:93–100. [PubMed: 15527767]
17. Kjellman C, et al. Identification and characterization of a human smad3 splicing variant lacking part of the linker region. Gene. 2004; 327:141–152. [PubMed: 14980711]
18. Jinnin M, Ihn H, Tamaki K. Characterization of SIS3, a novel specific inhibitor of Smad3, and its effect on transforming growth factor-beta1-induced extracellular matrix expression. Mol Pharmacol. 2006; 69:597–607. [PubMed: 16288083]
19. Dillon S, et al. A Toll-like receptor 2 ligand stimulates Th2 responses in vivo, via induction of extracellular signal-regulated kinase mitogen-activated protein kinase and c-Fos in dendritic cells. J Immunol. 2004; 172:4733–4743. [PubMed: 15067049]
20. Andre S, Tough DF, Lacroix-Desmazes S, Kaveri SV, Bayry J. Surveillance of antigen-presenting cells by CD4+ CD25+ regulatory T cells in autoimmunity: immunopathogenesis and therapeutic implications. Am J Pathol. 2009; 174:1575–1587. [PubMed: 19349365]
21. Werner F, et al. Transforming growth factor-beta 1 inhibition of macrophage activation is mediated via Smad3. J Biol Chem. 2000; 275:36653–36658. [PubMed: 10973958]
22. Li MO, Flavell RA. Contextual regulation of inflammation: a duet by transforming growth factor-beta and interleukin-10. Immunity. 2008; 28:468–476. [PubMed: 18400189]
23. Trotta R, et al. TGF-beta utilizes SMAD3 to inhibit CD16-mediated IFN-gamma production and antibody-dependent cellular cytotoxicity in human NK cells. J Immunol. 2008; 181:3784–3792. [PubMed: 18768831]
24. Musso T, et al. Transforming growth factor beta downregulates interleukin-1 (IL-1)-induced IL-6 production by human monocytes. Blood. 1990; 76:2466–2469. [PubMed: 2265243]
25. Larmonier N, et al. Tumor-derived CD4(+)CD25(+) regulatory T cell suppression of dendritic cell function involves TGF-beta and IL-10. Cancer Immunol Immunother. 2007; 56:48–59. [PubMed: 16612596]
26. Misra N, Bayry J, Lacroix-Desmazes S, Kazatchkine MD, Kaveri SV. Cutting edge: human CD4+CD25+ T cells restrain the maturation and antigen-presenting function of dendritic cells. J Immunol. 2004; 172:4676–4680. [PubMed: 15067041]
27. Bayry J, Triebel F, Kaveri SV, Tough DF. Human dendritic cells acquire a semimature phenotype and lymph node homing potential through interaction with CD4+CD25+ regulatory T cells. J Immunol. 2007; 178:4184–4193. [PubMed: 17371975]
28. Fogel-Petrovic M, et al. Physiological concentrations of transforming growth factor beta1 selectively inhibit human dendritic cell function. Int Immunopharmacol. 2007; 7:1924–1933. [PubMed: 18039529]
29. Laouar Y, et al. TGF-beta signaling in dendritic cells is a prerequisite for the control of autoimmune encephalomyelitis. Proc Natl Acad Sci USA. 2008; 105:10865–10870. [PubMed: 18669656]
30. Cohen I, et al. Differential release of chromatin-bound IL-1alpha discriminates between necrotic and apoptotic cell death by the ability to induce sterile inflammation. Proc Natl Acad Sci USA. 107:2574–2579. [PubMed: 20133797]
31. Werman A, et al. The precursor form of IL-1alpha is an intracrine proinflammatory activator of transcription. Proc Natl Acad Sci USA. 2004; 101:2434–2439. [PubMed: 14983027]
32. Carriere V, et al. IL-33, the IL-1-like cytokine ligand for ST2 receptor, is a chromatin-associated nuclear factor in vivo. Proc Natl Acad Sci USA. 2007; 104:282–287. [PubMed: 17185418]
33. Wilson KC, Cruikshank WW, Center DM, Zhang Y. Prointerleukin-16 contains a functional CcN motif that regulates nuclear localization. Biochemistry. 2002; 41:14306–14312. [PubMed: 12450396]
34. Yang H, Wang H, Tracey KJ. HMG-1 rediscovered as a cytokine. Shock. 2001; 15:247–253. [PubMed: 11303722]

35. Kleemann R, et al. Intracellular action of the cytokine MIF to modulate AP-1 activity and the cell cycle through Jab1. Nature. 2000; 408:211–216. [PubMed: 11089976]
36. Dinarello CA. Blocking IL-1 in systemic inflammation. J Exp Med. 2005; 201:1355–1359. [PubMed: 15867089]
37. Ross JA, Nagy ZS, Cheng H, Stepkowski SM, Kirken RA. Regulation of T cell homeostasis by JAKs and STATs. Arch Immunol Ther Exp (Warsz). 2007; 55:231–245. [PubMed: 17659375]
38. Ulloa L, Doody J, Massague J. Inhibition of transforming growth factor-beta/SMAD signalling by the interferon-gamma/STAT pathway. Nature. 1999; 397:710–713. [PubMed: 10067896]
39. Zauberman A, Lapter S, Zipori D. Smad proteins suppress CCAAT/enhancer-binding protein (C/EBP) beta- and STAT3-mediated transcriptional activation of the haptoglobin promoter. J Biol Chem. 2001; 276:24719–24725. [PubMed: 11331273]
40. Foster LC, et al. Role of activating protein-1 and high mobility group-I(Y) protein in the induction of CD44 gene expression by interleukin-1beta in vascular smooth muscle cells. FASEB J. 2000; 14:368–378. [PubMed: 10657993]
41. Imai K, Takeshita A, Hanazawa S. Transforming growth factor-beta inhibits lipopolysaccharide-stimulated expression of inflammatory cytokines in mouse macrophages through downregulation of activation protein 1 and CD14 receptor expression. Infect Immun. 2000; 68:2418–2423. [PubMed: 10768925]
42. Schieven GL. The biology of p38 kinase: a central role in inflammation. Curr Top Med Chem. 2005; 5:921–928. [PubMed: 16178737]
43. Martin M, Rehani K, Jope RS, Michalek SM. Toll-like receptor-mediated cytokine production is differentially regulated by glycogen synthase kinase 3. Nat Immunol. 2005; 6:777–784. [PubMed: 16007092]
44. McCartney-Francis N, Jin W, Wahl SM. Aberrant Toll receptor expression and endotoxin hypersensitivity in mice lacking a functional TGF-beta 1 signaling pathway. J Immunol. 2004; 172:3814–3821. [PubMed: 15004187]
45. Nold MF, et al. Endogenous IL-32 Controls Cytokine and HIV-1 Production. J Immunol. 2008; 181:557–565. [PubMed: 18566422]

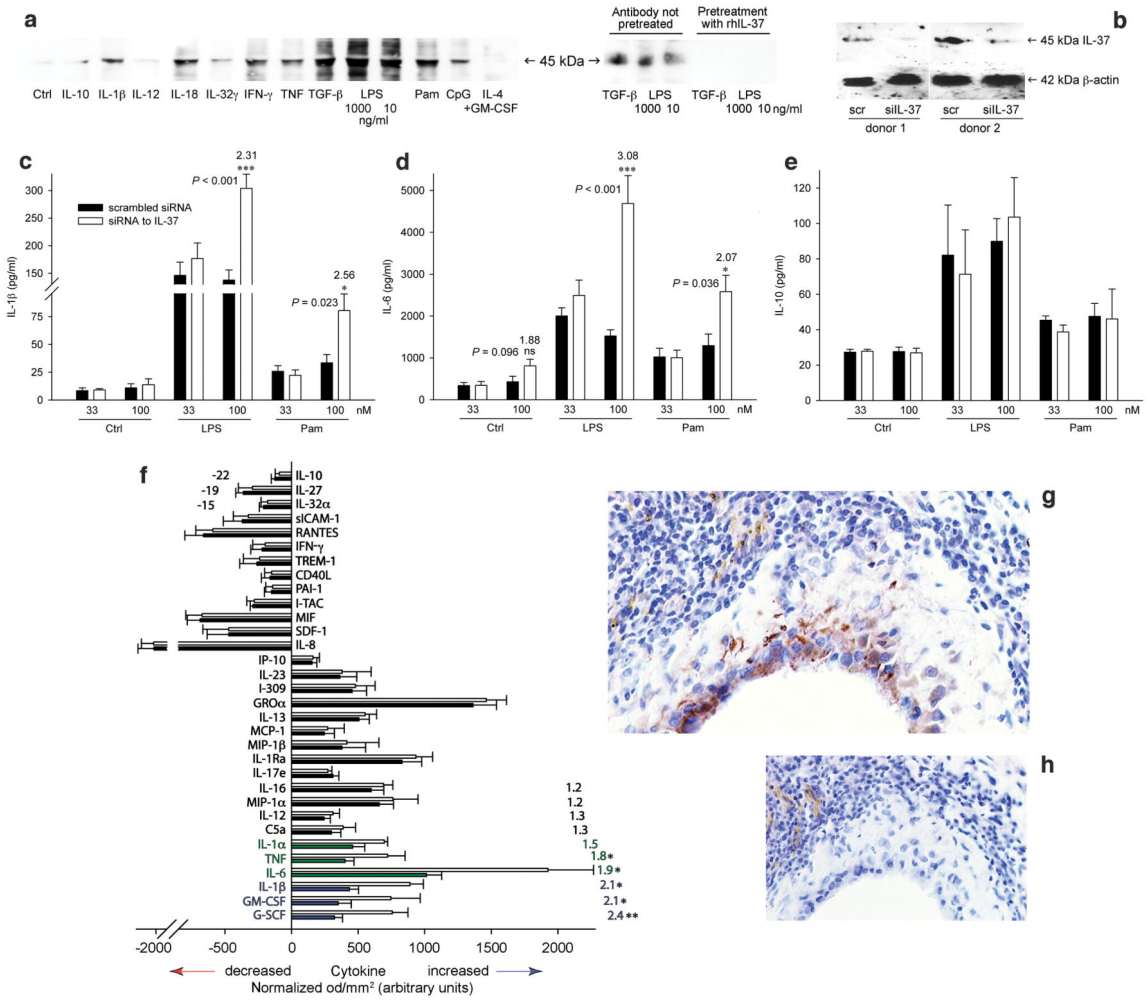


**Figure 1.**

Production and silencing of endogenous IL-37 in human PBMCs. (**a**, left) immunoblot of PBMC lysates after 20 h. One of 4 donors is depicted. Concentrations (ng/ml) are: IL-10, 25; IL-1β, 10; IL-12, 20; IL-18, 25; IL-32γ, 5; IFN-γ, 25; TNF, 20; TGF-$\beta_1$, 20; LPS as indicated; Pam, 10; CpG, 1000; IL-4, 20; GM-CSF, 40. (**a**, right) Before staining, anti-IL-37 was mixed with 1 μg/ml recombinant human IL-37b (right). (**b**) immunoblot of lysates from two donors 24 h after incubation with 1 μg/ml of LPS. 20 h prior, PBMCs were transfected with 100 nM of siIL-37 or scrambled siRNA. Two of five similar blots are shown. (**c**-**e**) 24 h after transfections, PBMCs were stimulated with 1 μg/ml LPS, 10 ng/ml $Pam_3CSK_4$, or left untreated for 24 h. Mean ± SEM concentrations of secreted IL-1β, IL-6, and IL-10 are shown ($n$ = 7; ns, not significant; *, $P < 0.05$; **, $P < 0.01$; and ***, $P < 0.001$ for siIL-37 compared to scrambled). The numbers above and next to the bars indicate fold changes and $P$-values, respectively. (**f**) PBMCs were transfected with either 100 nM siIL-37 (open bars) or scrambled siRNA (closed bars) and stimulated with 1 μg/ml LPS. After 24 h, pairs of siIL-37/scrambled siRNA from 3 donors were assessed by cytokine protein array. The graph depicts the results of densitometric analysis as normalized density/$mm^2$ ± SEM; *, $P < 0.05$; **, $P < 0.01$. Numbers indicate percent decrease or fold increase. Color code: Blue, mean

increase > 2-fold; green, mean increase 1.5- to 2-fold; black, small changes. (**g**) Immunohistochemical staining of IL-37 in synovial tissue from a rheumatoid arthritis patient with active disease. (**h**) Staining of the same tissue with a rabbit IgG control antibody. The panels are representative for 5 similar pairs of images.

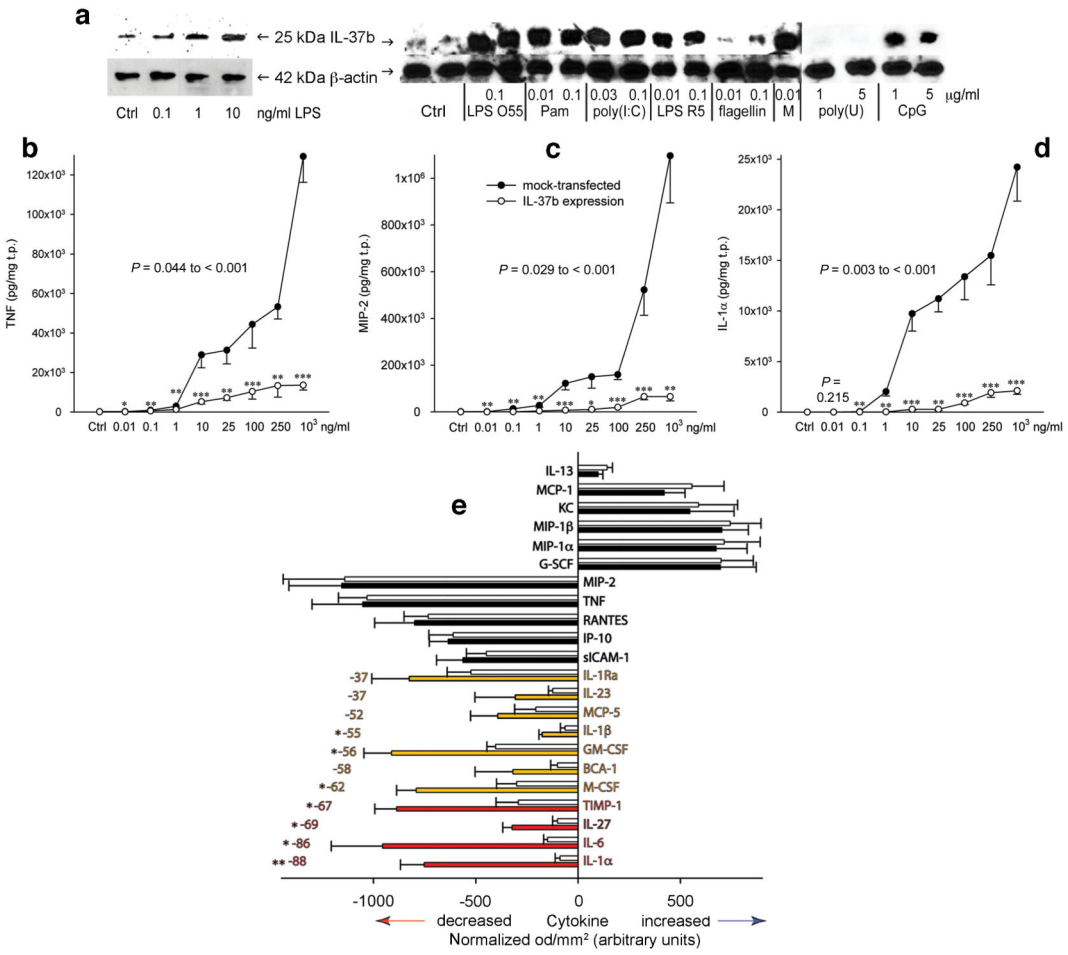


**Figure 2.**

Effect of TLR-induced IL-37b on cytokine production in RAW cells. (**a**) Immunoblots of RAW-IL-37 cells. Cells were incubated without (ctrl) or with increasing concentrations of LPS (left) or TLR ligands (right) for 24 h. Each blot represents one of four independently performed experiments. TLR ligands (in µg/ml) are indicated. Supernatants (**b,c**) or lysates (**d**) of LPS-stimulated cells were prepared. The panels depict means of absolute concentrations of cytokines normalized to total protein (t.p.) ± SEM, $n = 8$. Mock-transfected, filled symbols; RAW-IL-37 (= C17), open symbols; *, $P < 0.05$; **, $P < 0.01$; ***, $P < 0.001$ for RAW-IL-37 compared to mock-transfected. Absolute $P$-values are shown. IL-37b was absent in lysates of mock-transfected cells (not shown). (**e**) Protein array analysis of supernatants from RAW-IL-37 (open bars) and mock-transfected cells (closed bars) stimulated with LPS (100 ng/ml) for 24 h. Mean densities of RAW-IL-37 vs mock-transfected cells were obtained from 3 independently performed experiments. Results are shown as density/mm$^2$ ± SEM; *, $P < 0.05$; **, $P < 0.01$. Red indicates a mean reduction of more than 67%, orange symbolizes a decrease between 33 and 67%. Cytokines with little change are displayed by black bars.

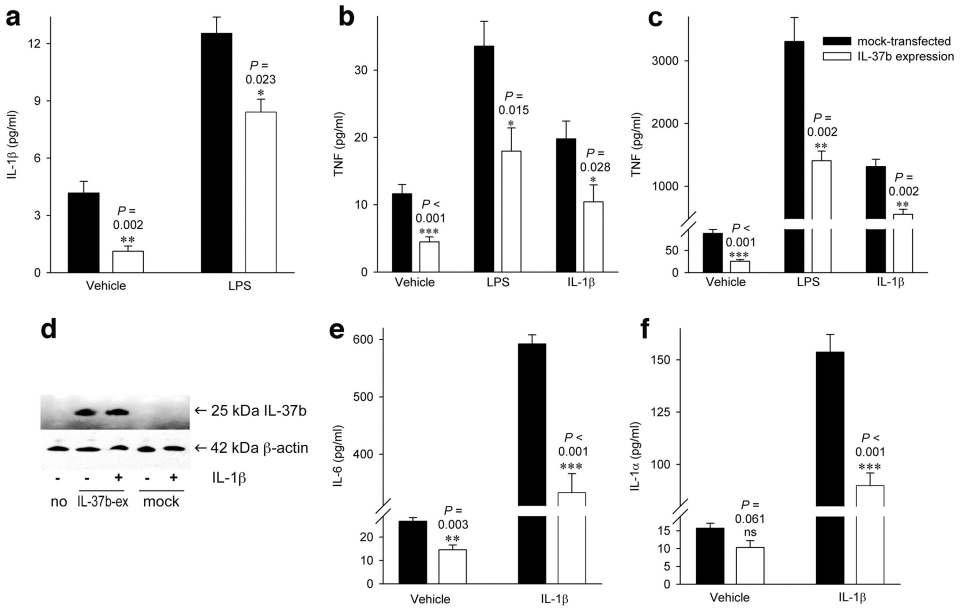


**Figure 3.**

Cytokine production in THP-1 (**a-c**) and A549 (**d-f**) cells transfected with IL-37b. Cells were transfected with either the pIRES-IL-37b plasmid or mock-transfected with pIRES lacking IL-37b. (**a,b**) IL-1β and TNF levels in undifferentiated, transiently transfected THP-1 stimulated with either 1 μg/ml LPS, 25 ng/ml IL-1β, or vehicle as indicated. (**c**) Absolute TNF levels in PMA-differentiated, transfected THP-1 stimulated with either LPS, IL-1β, or vehicle as indicated. (**a-c**) $n = 6$; *, $P < 0.05$; **, $P < 0.01$; ***, $P < 0.001$ for mock-transfected vs. IL-37b expression. Individual *P*-values are shown above the open bars. (**d-f**) A549 lung epithelial cells transfected in with either pIRES-IL-37b or mock transfected. (**d**) Immunoblot of IL-37b in non-transfected ("no") or transfected A549 cells; IL-37b-ex, IL-37b expression plasmid; mock, empty vector. One representative of four similar blots is shown. (**e,f**) IL-6 and IL-1α levels in IL-1β-stimulated (10 ng/ml) A549 cells following transfection with either the mock plasmid or the IL-37b construct. Absolute cytokine values (mean ± SEM) are indicated; n = 5; ns, not significant; **, $P < 0.01$; ***, $P < 0.001$. *P*-values are shown above the open bars.

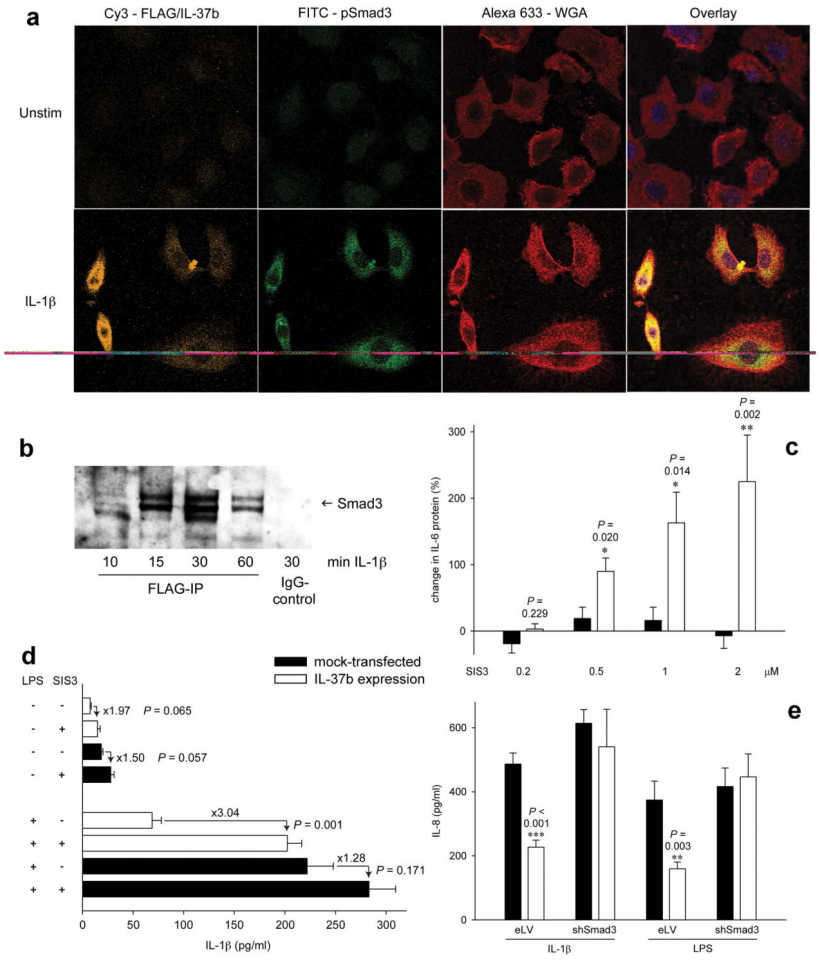


**Figure 4.**

Smad3 and IL-37. (**a**) Confocal microscopy of IL-37b-transfected A549 cells treated either with 10 ng/ml IL-1β or vehicle. Localization of IL-37b/FLAG (Cy3, yellow), phospho-Smad3 (FITC, green), cell membranes (Alexa Fluor 633, red), and nuclei (DAPI, blue, shown only in overlays) are shown. Bright yellow in the overlay images indicates colocalization. See Supplementary Fig. 3 for mock-transfected cells. (**b**) Anti-FLAG immunoprecipitation of IL-37b-transfected A549 cells stimulated with IL-1β (10 ng/ml) followed by non-reducing PAGE and immunoblotting with anti-Smad3. (**c,d**) SIS3 (in μM) was added to cultures of either RAW cell clones (**c**) or transfected and differentiated THP-1 macrophages (**d**) 30 min before the addition of LPS. IL-6 (**c**), and IL-1β (**d**) levels in culture supernatants after 24 h. (**c**) Mean ± SEM percent changes from LPS (100 ng/ml) alone, n = 6; *, $P < 0.05$ and **, $P < 0.01$ for RAW-IL-37 vs. mock-transfected cells. Numbers above open bars are *P*-values. (**d**) LPS and SIS3 were used at 1000 ng/ml and 2 μM, respectively. The graph depicts absolute IL-1β concentrations ± SEM, n = 4; numbers indicate fold-increases induced by SIS3 treatment and *P*-values. ns, not significant; **, $P < 0.01$ for increases in IL-1β production in mock-transfected vs. IL-37b-transfected THP-1 cells. (**e**) Mean ± SEM IL-8 in THP-1 cells stably transfected with shRNA to Smad3 (shSmad3) or scrambled (eLV) following transfection with the IL-37b construct or the control vector and

stimulated with 25 ng/ml IL-1β or 1000 ng/ml LPS (n = 4, **, $P < 0.01$ and ***, $P < 0.001$ for mock-transfected vs. IL-37b expression).

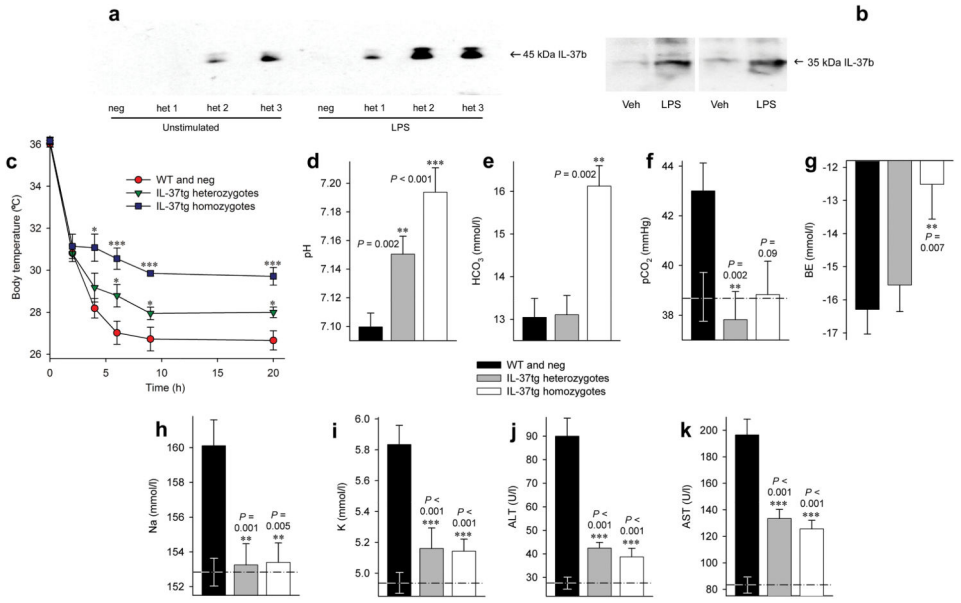


**Figure 5.**

Amelioration of endotoxic shock in mice transgenic for IL-37b. (**a**) Immunoprecipitation with anti-FLAG and anti-IL-37 and immunoblotting of lysates of splenocytes from several F1 generation IL-37tg and 4 PCR-negative littermates (neg). Splenocytes were incubated either with or without LPS (1 μg/ml) for 20 h. The data from one representative neg and three IL-37tg heterozygotes (het) are shown. (**b**) IL-37tg heterozygotes were injected with 10 mg/kg LPS or vehicle. 24 h later, peripheral blood was obtained and IL-37b was analyzed by immunoblotting. The panel shows staining against IL-37 from two representative pairs of vehicle- or LPS-injected mice. (**c**-**k**) 23 IL-37tg heterozygous, 10 homozygous, and 25 wild-type and neg mice were injected with 10 mg/kg LPS or vehicle. Means ± SEM are depicted; *, $P < 0.05$; **, $P < 0.01$; ***, $P < 0.001$ for wild-type and neg compared to IL-37tg as per one way ANOVA or one way ANOVA on ranks. The dash-dot lines indicate average levels in vehicle-injected IL-37tg, wild-type, and neg (between which no difference was observed) ± SEM, n = 5 heterozygotes, 3 homozygotes, and 5 neg-WT. (**c**) Body temperature was measured at the indicated time points. Actual *P*-values: IL-37tg homozygotes: 4 h, 0.025; 6, 9, and 24 h, < 0.001; IL-37tg heterozygotes: 6 h, 0.029; 9 h, 0.046; 24 h, 0.022. (**d**-**k**) After 24 h, plasma was harvested and blood gases (**d**-**g**), electrolytes (**h**,**i**), and liver enzymes (**j**,**k**) were determined.

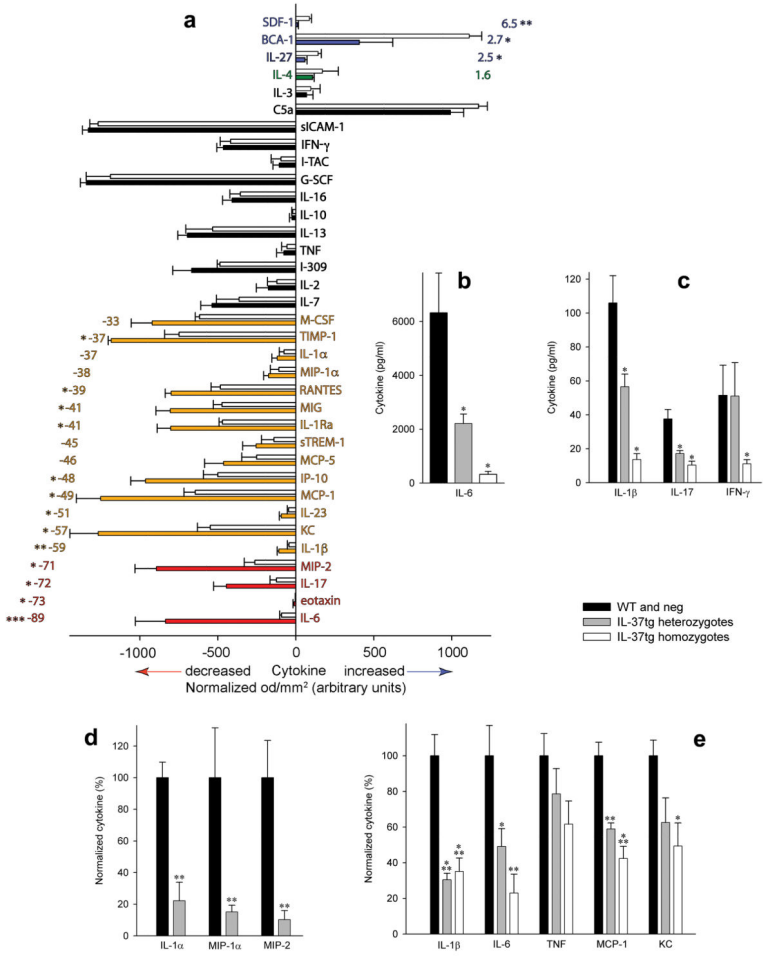


**Figure 6.**

Production of LPS-induced cytokines in IL-37tg mice. IL-37tg as well as wild-type and neg mice were injected with 10 mg/kg LPS or vehicle. 24 h later, plasma (**a-c**) and lungs (**d, e**) were obtained and analyzed by electrochemiluminescence assay or ELISA (**b-e**), or protein array (**a**). The mice used to create Fig. 6 are identical with those used for Fig. 5. (**a**) Protein array analysis was performed on the plasma of three IL-37tg heterozygous (open bars) and four wild-type or neg (closed bars) mice. The results of the densitometry are depicted as normalized density/mm$^2$ ± SEM; *, $P < 0.05$; **, $P < 0.01$; ***, $P < 0.001$. Numbers indicate percent decrease or fold increase. Color code: Red, mean decrease > 67%; orange, mean decrease 33 to 67%; black, small changes (−33% decrease to +50% or 1.5-fold increase); green, 1.5- to 2-fold increase; blue, > 2-fold increase. (**b-e**) The graphs depict absolute values ± SEM in 23 IL-37tg heterozygotes, 10 homozygotes, and 25 wild-type and neg mice; *, $P < 0.05$; **, $P < 0.01$; ***, $P < 0.001$ for IL-37tg het or hom vs neg-WT. For all individual *P*-values in this Figure and statistical tests performed, see Supplementary Table 2.

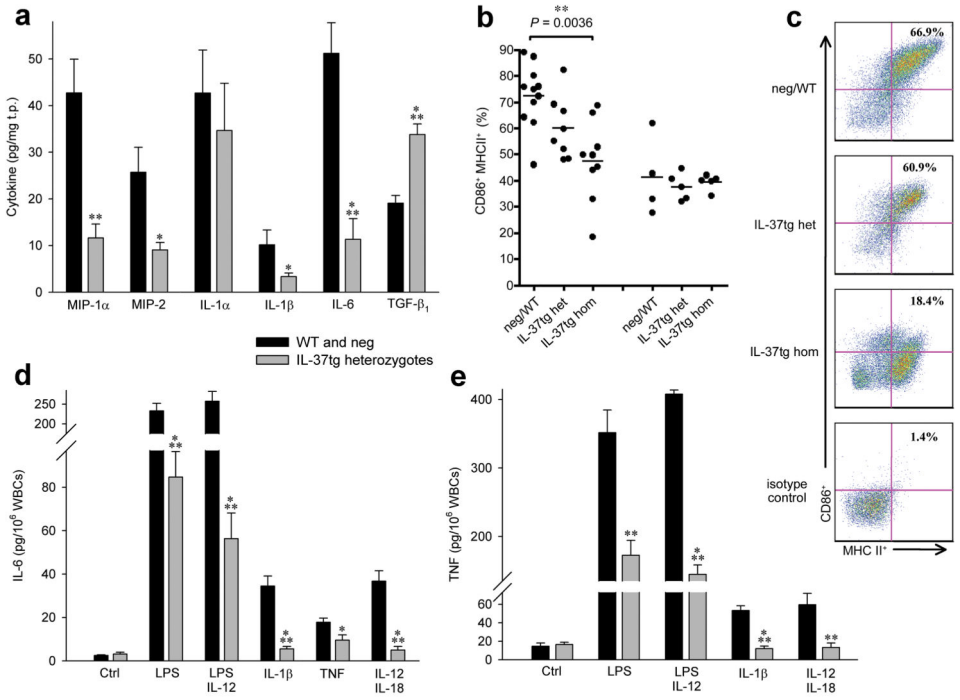


**Figure 7.**

Cytokines and DC activation in IL-37tg and neg-WT spleens and whole blood. (**a-c**) Spleens were harvested from the same mice shown in Fig. 6 (i.e. 24 h after injection of 10 mg/kg LPS or vehicle) and either lysed and analyzed for cytokine levels (**a**) or incubated with collagenase IV, stained, and subjected to flow-cytometry (**b,c**). (**a**) Electrochemiluminescence and ELISA measurements of the indicated cytokines depicted as cytokine concentration ± SEM normalized to total protein (t.p.); *, $P < 0.05$; **, $P < 0.01$; ***, $P < 0.001$; actual *P*-values: MIP-1α, 0.002; MIP-2, 0.014; IL-1α, 0.28; IL-1β, 0.021; IL-6 and TGF-$\beta_1$ < 0.001. (**b,c**) $CD11c^+$ DC were identified in the viable splenocytes and then analyzed for expression of CD86 and MHC II; $n = 11$ LPS and 4 vehicle neg-WT, 8 LPS and 5 vehicle IL-37tg heterozygotes (het), and 9 LPS and 5 vehicle IL-37tg homozygotes (hom); **, $P < 0.01$ for neg-WT vs IL-37tg hom. (**b**) Statistical assessment of DC activation displayed as $CD86^+MHC\ II^+$ DC among total DC in percent in LPS- and vehicle-injected mice. Horizontal lines show means. (**c**) Exemplary scatter plot of one LPS-injected mouse from each strain. Percent of CD86/MHC II double-positive cells is indicated in right upper corner. (**d,e**) Whole blood was obtained from IL-37tg heterozygotes and neg-WT, was stimulated as indicated (concentrations in ng/ml: LPS, 1000; IL-12, 20; IL-1β, 20; TNF, 20; IL-18, 50), and incubated for 20 h. The data depict mean ± SEM of absolute cytokine concentrations in picograms per million white blood cells. n = 6 IL-37tg and 8 neg-WT; *, $P < 0.05$; **, $P < 0.01$; ***, $P < 0.001$ for neg-WT vs. IL-37tg; actual *P*-values: (**d**) all < 0.001 except Ctrl, 0.65 and TNF, 0.04. (**e**) Ctrl, 0.58; LPS, 0.001; LPS plus IL-12 and IL-1β, < 0.001; IL-12 plus IL-18, 0.004.

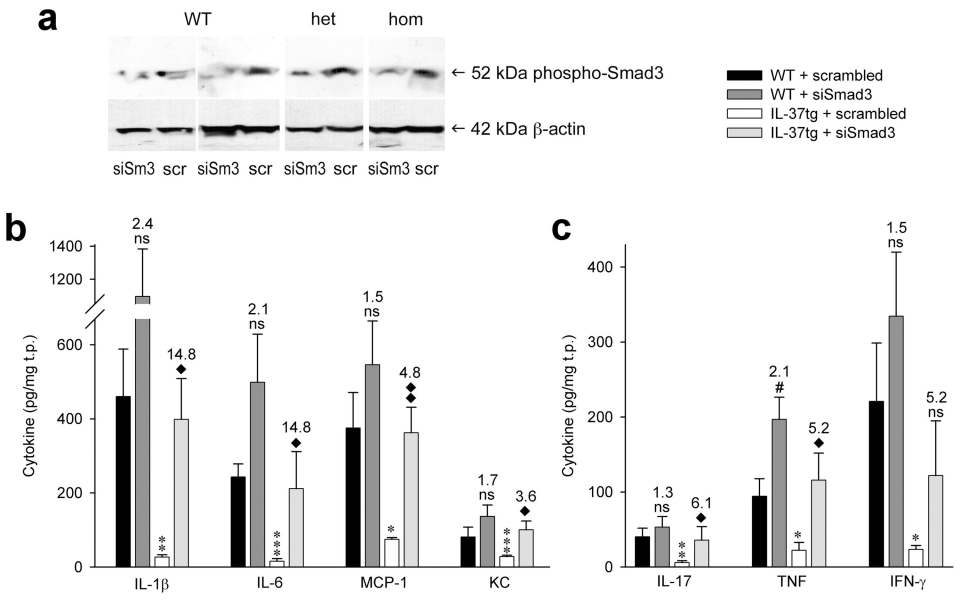


**Figure 8.**

Silencing of Smad3 reduces the activity of IL-37 *in vivo*. IL-37tg and neg-WT mice inhaled 3 μg/g of either scrambled siRNA (scr) or siRNA to Smad3 (siSm3). 20 h later, each mouse inhaled 3 μg/g LPS. After another 18 h, lungs were harvested and assayed for production of Smad3 (**a**) and cytokines (**b, c**). (**a**) Phospho-Smad3 was assessed by immunoblotting. Four representative pairs of mice are shown. (**b, c**) Absolute concentrations of each cytokine per mg total protein (t.p.) ± SEM are shown. n = 8 for each group, i.e. for neg-WT + scrambled, neg/WT + siSmad3, IL-37tg + scrambled, and IL-37tg + siSmad3. ns, not significant; *, $P < 0.05$; **, $P < 0.01$; ***, $P < 0.001$ for IL-37tg + scrambled vs neg-WT + scrambled and ◆, $P < 0.05$; ◆◆, $P < 0.01$ for IL-37tg + scrambled vs IL-37tg + siSmad3. Numbers indicate fold-increases conferred by treatment with siSmad3, i.e. comparing scrambled to siSmad3 in neg-WT and IL-37tg. *P*-values are listed in Supplementary Table 3.